Earth and Planetary Science Letters 459 (2017) 127–135

Contents lists available at ScienceDirect

Earth and Planetary Science Letters

www.elsevier.com/locate/epsl

Using GPS and absolute gravity observations to separate the effects of present-day and Pleistocene ice-mass changes in South East Greenland

T. van Dam *, O. Francis, J. Wahr, S.A. Khan, M. Bevis, M.R. van den Broeke

University of Luxembourg, Luxembourg

ARTICLE INFO

Article history:
Received 23 November 2015
Received in revised form 20 September 2016
Accepted 3 November 2016
Available online 1 December 2016
Editor: B. Buffett

Keywords:
Greenland
GIA
present day ice melting
crustal uplift
GPS
absolute gravity

ABSTRACT

Measurements of vertical crustal uplift from bedrock sites around the edge of the Greenland ice sheet (GrIS) can be used to constrain present day mass loss. Interpreting any observed crustal displacement around the GrIS in terms of present day changes in ice is complicated, however, by the glacial isostatic adjustment (GIA) signal. With GPS observations alone, it is impossible to separate the uplift driven by present day mass changes from that due to ice mass changes in the past. Wahr et al. (1995) demonstrated that viscoelastic surface displacements were related to the viscoelastic gravity changes through a proportionality constant that is nearly independent of the choice of Earth viscosity or ice history model. Thus, by making measurements of both gravity and surface motion at a bedrock site, the viscoelastic effects could be removed from the observations and we would be able to constrain present day ice mass changes. Alternatively, we could use the same observations of surface displacements and gravity to determine the GIA signal. In this paper, we extend the theory of Wahr et al. (1995) by introducing a constant, Z, that represents the ratio between the elastic changes in gravity and elastic uplift at a particular site due to present day mass changes. Further, we combine 20 yrs of GPS observations of uplift with eight absolute gravity observations over the same period to determine the GIA signal near Kulusuk, a site on the southeastern side of the GrIS, to experimentally demonstrate the theory. We estimate that the GIA signal in the region is 4.49 ± 1.44 mm/yr and is inconsistent with most previously reported model predictions that demonstrate that the GIA signal here is negative. However, as there is very little in situ data to constrain the GIA rate in this part of Greenland, the Earth model or the ice history reconstructions could be inaccurate (Khan et al., 2016). Improving the estimate of GIA in this region of Greenland will allow us to better determine the present day changes in ice mass in the region, e.g. from GRACE.

1. Introduction

Precise estimates of the present-day rates and accelerations of ice-mass loss from the polar ice-sheets are important for predicting potential changes in sea level. Current predictions of 21st century sea level change are limited by, among other things, their ability to precisely capture the effects of global warming on the Greenland ice sheet (GrIS.)

One method for constraining the mass loss on the GrIS is to make measurements of vertical crustal uplift rates from bedrock locations around the edge of the ice sheet. As the ice mass decreases, the Earth's surface displaces elastically upward to an extent that is proportional to the amount of mass that is lost. Various investigators have used this approach to examine changes in mass of the GrIS (Jiang et al., 2010; Khan et al., 2010, 2013, 2016; Nielsen et al., 2012; Bevis et al., 2012; Wahr et al., 2013). These results demonstrate the value of using crustal motions to constrain estimates of mass change.

However, the interpretation of any observed crustal displacement around the GrIS is complicated by the Glacial Isostatic Adjustment (GIA) signal: the Earth's slower viscoelastic response to past changes in the ice mass load. The magnitude of the GIA uplift is a function of the temporal history of the ice load and the Earth's viscosity profile (Peltier, 2002; Tarasov and Peltier, 2002; Huybrechts, 2002; Fleming and Lambeck, 2004; A et al., 2013). Using only GPS observations of crustal displacement, it is impossible to separate the uplift driven by present day mass changes from that due to ice mass changes in the past, e.g. the extensive retreat of the ice sheets since the Last Glacial Maximum (LGM) or even ice sheet changes during the Little Ice Age.

Using the VM-2 viscosity profile and ICE-5G ice load history from Peltier (2004), A et al. (2013) predicted the GIA displacement

* Corresponding author.
E-mail address: tonie.vandam@uni.lu (T. van Dam).

http://dx.doi.org/10.1016/j.epsl.2016.11.014
0012-821X/

in the region of Kulusuk should be −0.7 mm/yr. However, this signal could easily be much larger or smaller depending on the choice of Earth model or ice load history (Argus et al., 2014). GPS stations located on bedrock in southeast Greenland show that the surface is uplifting at rates on the order of 10.0 mm/yr (Bevis et al., 2012). An error in the prediction of the GIA component would bias our estimate of present-day mass loss.

The problem of separating the elastic from viscoelastic surface displacements in GPS time series from Greenland or Antarctica was first addressed by Wahr et al. (1995). In that publication, the authors demonstrated that viscoelastic surface displacements were related to the viscoelastic gravity changes through a proportionality constant that is nearly independent of the choice of Earth viscosity or ice history model. Thus, by making measurements of both gravity and surface motion at a bedrock site, the viscoelastic effects could be removed from the observations and we would be able to constrain present day ice mass changes. Alternatively, we could use the same observations of surface displacements and gravity to determine the GIA signal.

The theoretical work by Wahr et al. (1995) assumed that the changes to present day gravity and uplift would be coherent over long spatial wavelengths. Altimetric observations show that the change in the surface of the ice is not necessarily coherent in space. So that we must find a way to relate elastic changes in gravity and uplift at any location. In this paper, we extend the theory outlined in Wahr et al. (1995) by assuming a constant ratio between elastic uplift and elastic gravity changes in southeast Greenland. We use a surface mass balance model (van Meijgaard et al., 2008; Noël et al., 2015) for the ice sheet, as well as a gridded model of ice sheet elevations derived from satellite and airborne observations, and estimate this ratio to be $Z = -0.279 \pm 0.01$ μGal/mm at Kulusuk. We then use Z to separate the effects of elastic uplift and GIA in Greenland. Estimates of Z depend on the site location and on the spatial distribution of the load. Our value of Z is only valid for Kulusuk.

Our observations of surface uplift and absolute gravity extend from 1996 to 2013. In 1996 we installed a permanent GPS receiver, KULU, near Kulusuk Airport in southeast Greenland. In the last eighteen years, we have taken ten absolute gravity observations at that site of which only eight were used in our calculations. We find that our observations and theory predict a positive GIA contribution to surface uplift. This positive trend disagrees with most published GIA estimates for the region, which are negative.

2. Theory

We begin by assuming that there are only two possible sources of secular signals in the observed uplift and gravity: the Earth's elastic response to present-day ice variability, and the GIA signal. We can then describe the secular trends in uplift and gravity as:

$$\delta\dot{u} = \delta\dot{u}_{ice} + \delta\dot{u}_{GIA} \tag{1a}$$

$$\delta\dot{g} = \delta\dot{g}_{ice} + \delta\dot{g}_{GIA}, \tag{1b}$$

where the subscript "ice" refers to the elastic response of the Earth to present-day ice variability, and where a dot above a variable indicates the secular trend of that variable. We assume the units of $\delta\dot{u}$ and $\delta\dot{g}$ are mm/yr and μGal/yr, respectively, and that gravity increases as the surface moves closer to the center of the Earth.

The trend in the gravitational acceleration at a point on the Earth's surface can be separated into two components, $\delta\dot{g} = \delta\dot{g}_u + \delta\dot{g}_m$, where $\delta\dot{g}_u$ represents the effects of vertical displacements of the surface responding to loading and $\delta\dot{g}_m$ that is caused by changes in the mass distribution of the ice load and in the underlying Earth. The relation between $\delta\dot{g}_u$ and the trend in the surface displacement is given by the standard free-air gravity effect: $\delta\dot{g}_u = -0.31$ μGal/mm $\times\ \delta\dot{u}$. For the GIA signal, Wahr et al. (1995) considered a number of deglaciation models and viscosity profiles, and found that in all cases the GIA mass change gravity effect and the GIA uplift can be related to one another using the approximation $\delta\dot{g}_{m\_GIA} \approx \frac{1}{6.5}$ μGal/mm $\times\ \delta\dot{u}_{GIA}$, so that

$$\delta\dot{g}_{GIA} = \delta\dot{g}_{u_{GIA}} + \delta\dot{g}_{m_{GIA}} = -0.31 \times \delta\dot{u}_{GIA} + \frac{\delta\dot{u}_{GIA}}{6.5} \tag{2}$$

Recall that our goal is to use observations of $\delta\dot{u}$ and $\delta\dot{g}$ to determine $\delta\dot{u}_{GIA}$ and $\delta\dot{u}_{ice}$. Equation (2) allows us to relate $\delta\dot{g}_{GIA}$ in (1b) to $\delta\dot{u}_{GIA}$. If we can find a similar relationship between $\delta\dot{g}_{ice}$ and $\delta\dot{u}_{ice}$, then we can eliminate $\delta\dot{g}_{ice}$ and $\delta\dot{g}_{GIA}$ from (1), and use our observations to solve for $\delta\dot{u}_{GIA}$ and $\delta\dot{u}_{ice}$.

Let the variable Z represent the ratio of the gravity signal to the uplift signal caused by the Earth's elastic response to present-day loading, so that

$$\delta\dot{g}_{ice} = Z\delta\dot{u}_{ice}. \tag{3}$$

The gravity signal in this case includes both the contribution caused by vertical displacements, $\delta\dot{g}_{u_{ice}}$, and the contribution caused by changes in the mass of both the load and the load-induced deformation of the Earth, $\delta\dot{g}_{m_{ice}}$. Unlike the $(-0.31 + 1/6.5)$ factor in Equation (2), that describes a similar relationship for the Earth's viscoelastic response to past loading, the factor Z can depend significantly on how the load is distributed relative to the site where the observations are made.

Suppose we know Z (in μGal/mm). (In the next section we will discuss how Z is determined.) Using Equation (2) and our definition of Z, Equation (1) can be rewritten as

$$\delta\dot{g} = \delta\dot{g}_{ice} + \delta\dot{g}_{GIA} = Z\delta\dot{u}_{ice} + \frac{1}{6.5}\delta\dot{u}_{GIA} - 0.31\delta\dot{u}_{GIA}. \tag{4}$$

Substituting Equation (1a) into Equation (4) gives:

$$\frac{\delta\dot{g}}{Z} - \delta\dot{u} = \left[-1 + \frac{\frac{1}{6.5} - 0.31}{Z}\right]\delta\dot{u}_{GIA}$$

or

$$\frac{\delta\dot{g}}{Z} - \delta\dot{u} = (A-1)\delta\dot{u}_{GIA}, \tag{5}$$

where $A = [\frac{1}{6.5 \times Z} - \frac{0.31}{Z}] = \frac{-0.156}{Z}$.

Using Equation (5), we see that the value of $\delta\dot{u}_{GIA}$ can be derived from the uplift and gravity observations as:

$$\delta\dot{u}_{GIA} = \frac{1}{A-1}\left[\frac{\delta\dot{g}}{Z} - \delta\dot{u}\right]. \tag{6}$$

When we put this value for $\delta\dot{u}_{GIA}$ into Equation (1a), we can get an estimate for $\delta\dot{u}_{ice}$ as well.

2.1. Calculating the scaling factor, Z

We don't know what the true load looks like; if we did, then we could model the Earth's elastic response to that load and remove it from the GPS measurements to infer the GIA signal – without having to include the gravity measurements at all. We do have access to some plausible models of how the present day ice load is changing with time across Greenland, and we can use those models to obtain an estimate of Z and to see how sensitive that estimate is to different assumptions about the load distribution.

First, suppose the only surface loads that have a significant impact on either the secular uplift rate or the secular change in gravity at KULU are caused by mass changes on the Greenland ice sheet. We place a unit mass load at a single location on the ice sheet. Then we use mass-loading Green's functions derived for

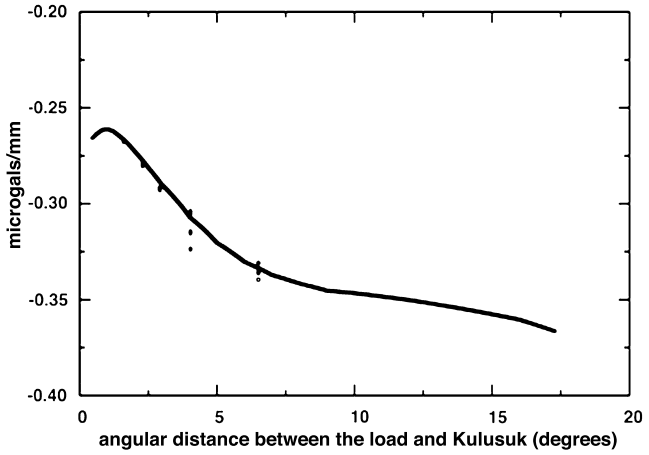

Fig. 1. The ratio of predicted gravity change to uplift, Z, at KULU due to a load at a given angular distance for a single epoch of RACMO2 data (279181 points each represented as an unfilled circle). The load is assumed to be a change in mass at each point equivalent to 50 mm. The absolute value Z increases rapidly with distance from KULU. The points that do not fall on the line in the image are outliers.

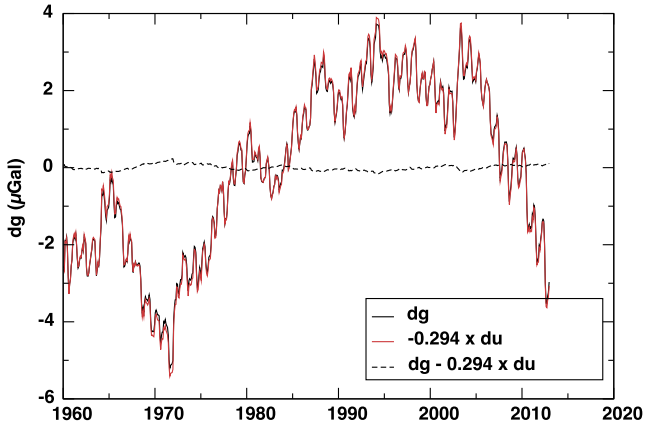

Fig. 2. Gravity, δg_{ice} (black line) and $(-0.294\ \mu\text{Gal/mm} \times \delta u_{ice}) = (Z \times \delta u_{ice})$ at KULU (red line). δg_{ice} and δu_{ice} are computed for each epoch of observations using mass variations predicted by the RACMO2 model, and using the load Green's functions based on PREM (red line). The black dashed line is the difference between the two curves. This figure demonstrates that our initial estimate of Z is robust over an extensive period of time.

a PREM Earth model (method described in Francis and Mazzega, 1990; various tidal models tested) to determine the change in gravity and the surface displacement due to the point load. We compute the resulting uplift and gravity signals at KULU, and take the ratio to get Z. We do this for a load at each point, one at a time, of a 10.9 km × 10.9 km latitude/longitude grid that covers the ice sheet.

The results for Z, as a function of the angular distance from KULU, are shown in Fig. 1. The value of Z varies between -0.25 and -0.38 μGal/mm. This is a wide range for Z, and so might suggest that we are unlikely to find a single value of Z that would work for all plausible loading models. But the loading points that contribute the most to the uplift and gravity signals at KULU are the points that are both close to KULU and that have large secular mass variations. These points will have the greatest impact on the cumulative value of Z. And, the loading at points far from KULU have will relatively little impact on the cumulative value of Z, which means the large Z values shown in Fig. 1 are largely irrelevant. This constrains the range of possible Z values considerably, and suggests it might be possible to describe the gravity-to-uplift ratio with a value of Z that can be estimated without knowing the exact loading distribution. This assumption will be explored in detail in the following section.

The formulation in the section above is based on the assumption that we can obtain a good estimate of the scaling factor, Z (in Equation (3)), without precise knowledge of the secular mass changes. We estimate Z by modelling the elastic uplift and gravity change caused by models of the evolving surface ice/snow load. We use two such models. One estimate of Z is derived from the GrIS surface mass balance (SMB) that was calculated using the Regional Atmospheric Climate Model (RACMO2/GR) (Noël et al., 2015) of the GrIS. The other estimate is based on satellite and airborne laser altimetry observations.

Output from the RACMO2/GR SMB model consists of monthly estimates of net snow/ice accumulation rates from a 53-year climate simulation (1960–2012) at high horizontal resolution (∼11 km). For Greenland, RACMO2 has been coupled to a physical snow model that treats surface albedo as a function of snow/firn/ice properties and includes meltwater percolation, retention, and refreezing (Ettema et al., 2009). The modeled SMB agrees well with in situ observations (Noël et al., 2015) as well as with mass estimates obtained using data from the Gravity Recovery and Climate Experiment (van den Broeke et al., 2009; Rignot et al., 2011).

RACMO2 does not include contributions from glacier dynamics, or from any other horizontal displacements of mass, anywhere in the ice sheet, that tend to move snow and ice downslope toward the margins. If the ice sheet were in long-term balance, then at every grid point the mass change caused by the horizontal transport would offset the mass change caused by the net accumulation at that point when both those mass changes are averaged over a long time span. The GrIS has been losing mass and so has been out of balance over at least the last decade and probably longer. Still, we have included the effects of horizontal mass transport in our analysis by assuming it is constant in time and that its value at each grid point exactly offsets the 1960–2012 average accumulation rate at that grid point. This is accomplished by computing the 1960–2012 mean of the net accumulation rate at each grid point and removing that mean from the time series of monthly accumulation rates at that point. We then integrate the resulting, demeaned monthly rates over time to obtain a time series of monthly, gridded mass variations.

We convolve those gridded mass fields with load Green's functions to obtain time series for the uplift, $\delta u_{ice}(t)$, and the gravity change, $\delta g_{ice}(t)$, for each epoch of the model at KULU. An estimate of Z can be obtained by then comparing the trends in $\delta u_{ice}(t)$ and $\delta g_{ice}(t)$. We use two sets of Green's functions, one from Farrell (1972) for the Gutenberg–Bullen A structural model and PREM from Francis and Mazzega (1990), Dziewonski and Anderson (1981) to allow us to assess the possible impact of Green's function errors on the results (to be discussed later).

We use the 53-year RACMO2 data set to determine the best-fitting scale factor between the gravity perturbation and the uplift. We least squares fit an annual signal and trends to both $\delta u_{ice}(t)$ and $\delta g_{ice}(t)$. We obtain $Z' = \delta\dot{g}_{ice}/\delta\dot{u}_{ice} = -0.294 \pm 0.02$ μGal/mm, where ± 0.02 is the formal uncertainty estimate. (Please note, the prime on our value of Z indicates that this is not our final value of Z nor its uncertainty.)

The ratio, $\delta g_{ice}(t)/\delta u_{ice}(t)$ at any time step depends solely on the spatial pattern of the load at that time step. Fig. 2 compares $\delta g_{ice}(t)$ (solid black line) and $(-0.294\ \mu\text{Gal/mm} \times \delta u_{ice}(t))$ (red line) from 1960 to the end of 2012. The two curves are in good agreement; the RMS of the difference between them (dotted black line) is 0.07 μGal, compared with an RMS of 2.2 μGal for $\delta g_{ice}(t)$ alone (solid black line). The fact that there is such good agreement

Table 1
Summary of determinations of Z.

	Z (μGal/mm)	Z (μGal/mm) with elevation of mass
RACMO2 (1998.5–2003.5)	-0.250 ± 0.51	-0.223 ± 0.48
RACMO2 (2003.5–2012.5)	-0.285 ± 0.01	-0.273 ± 0.01
Weighted Mean of RACMO2	-0.285 ± 0.01	-0.273 ± 0.01
Weighted Mean of RACMO2 estimates[2]		-0.274 ± 0.01
Altimetry (ICESat, LVIS, ATM)		-0.280 ± 0.00[1]
Weighted Mean of RACMO2 + Altimetry estimates[2]		-0.279 ± 0.01

[1] No error estimate on this value.
[2] Error on the weighted mean takes into account the absolute differences of the values themselves.

between $\delta g_{ice}(t)$ and -0.294 μGal/mm $\times \delta u_{ice}(t)$ at all months and all periods (e.g. seasonal, interannual, decadal, etc.), even though the spatial patterns of the mass loads are certain to be different for different months and periods, is an indication that a single value of $Z' \approx 0.294$ μGal/mm provides a good estimate of the ratio of gravity to uplift for a wide range of plausible SMB spatial patterns. And, it suggests that if the only mass variations were caused by SMB, then $Z = Z'$ in Equation (3) (the ratio of the secular trends in gravity and uplift) is likely to also have about this same value.

As for the effects of the Green's functions on our estimate of Z', the difference between the value of Z' estimated using the Gutenberg Bullen Green's functions and the value estimated using the PREM Green's functions is far smaller than the formal uncertainty on the estimate of Z'. We conclude that errors in the Green's functions are not a significant source of uncertainty in our final estimate of Z'.

Rather than use the value $Z' = 0.294$ μGal/mm as the final value, we repeat the fit but using the $\delta u_{ice}(t)$ and $\delta g_{ice}(t)$ values only over the time spans for which we have absolute gravity and continuous GPS data: 1998.5–2003.5 and 2003.5–2012.5. (The logic behind our choice of these time periods will be discussed in detail in Section 3 and 4. In short, the uplift rate increases after 2003.5 requiring a new estimate of GPS and absolute gravity observations.) After removing the annual signal from the gravity and uplift predictions over these periods, we find the best fitting values of Z are $Z = -0.250 \pm 0.51$ and $Z = -0.285 \pm 0.01$ for the two time spans respectively where the errors represent the formal uncertainties (Table 1). The weighted mean of these two RACMO2 based estimates of Z is equal to -0.285 ± 0.01 μGal/mm.

Our RACMO2 value of Z does not include the effect of the elevation of the ice mass change on our estimates of Z (Mémin et al., 2012). We recalculate Z using the actual height of the elevation change of the ice mass. In this case, we estimate a value of $Z_{elev} = -0.223 \pm 0.48$ and $Z_{elev} = -0.273 \pm 0.01$ μGal/mm for the two time periods. We average these values of Z_{elev} in a weighted sense to our previous values of Z for the two time periods to obtain $Z = -0.279 \pm 0.01$ μGal/mm as our best estimate of Z as determined from the RACMO2 SMB model.

This tentative value of Z, though, is based solely on the SMB mass load, and does not include the impact of dynamic changes in GrIS glaciers. There are large, rapidly evolving glaciers close to KULU (e.g. Helheim and Kangerdlussuaq glaciers, as well as systems of smaller glaciers to the north and southwest), and these could contribute significantly to both $\delta u_{ice}(t)$ and $\delta g_{ice}(t)$.

To consider the combined effects of dynamic glacier signals and SMB variations, we use a gridded model of the 2003–2012 secular mass trend over the GrIS, derived from three types of laser altimetry observations of elevation change. These include high-resolution Ice, Cloud and land Elevation Satellite (ICESat) data (Zwally et al., 2011) during 2003–2009, Land, Vegetation and Ice Sensor (LVIS) data (Blair and Hoften, 2012) during 2007–2012, and 2003–2012 altimeter surveys from NASA's ATM flights (Krabill, 2011). For ICESat we use GLA12 Release 31 data, and correct for the inter-campaign bias using the biases listed in Table 3 Column 4 of Siegfried et al. (2011). The inter-campaign biases were derived over the global oceans by comparing them to a mean sea surface topography model based on TOPEX/Poseidon.

ICESat elevations have a single-shot uncertainty of $\sigma_{ICESAT} = 0.2$ m, and ATM data have an elevation uncertainty of $\sigma_{ATM} = 0.1$ m. The single-shot accuracy of LVIS data is $\sigma_{LVIS} = 0.1$ m. The procedure for deriving ice surface elevation changes is described in detail by Khan et al. (2013), and is similar to the method used by, for example, Ewert et al. (2012), Smith et al. (2009), and Kjeldsen et al. (2013). We use the observed ice elevation change rates to interpolate (using collocation) ice-thinning values into a regular grid of 2.5×2.5 km.

These altimeter-based, secular trends in elevation include contributions from both SMB and dynamic thinning or thickening of glaciers. The resulting mass trends are convolved with the loading Green's functions, to estimate $\delta \dot{g}_{ice}$ and $\delta \dot{u}_{ice}$ at KULU. The ratio of these two trends at KULU is $Z_{ALT} = -0.280$ μGal/mm, which agrees with the ratio obtained above using the SMB loading results.

Finally, although the altimeter-based mass trends, above, include both the SMB and dynamic glacier signals, we consider one final mass load model where we add an independent dynamic glacier estimate for Helheim and Kangerdlugssuaq glaciers to the RACMO2 SMB fields. Helheim is located approximately 90 km NNW of KULU; Kangerdlugssuaq is 400 km NNE. To determine what, if any, contribution mass changes on these glaciers might have on our estimate of Z, we add an estimate $\delta \dot{g}_{ice}$ and $\delta \dot{u}_{ice}$ from these glaciers to the RACMO2 SMB values for $\delta \dot{g}_{ice}$ and $\delta \dot{u}_{ice}$ and then we recompute Z. We use realistic estimates of the change in ice elevation from Howat et al. (2011) and Csatho et al. (2014). The rate of change of the ice elevation has not been constant over the period 1998.5–2011. However, as we are only trying to obtain an approximate estimate of the effect, the assumption of a constant rate of change is sufficient. We use a density of 917 kg/m^3 for the ice to get a mass change. We then assume the change in ice is constant over the area of the basin (the area of the drainage basin is obtained from Rignot and Kanagaratnam (2006)). We find that changes on Helheim alone, Kangerdlugssuaq alone, and Helheim and Kangerdlugssuaq together, affect our estimate of Z computed using the SMB fields alone, by 0.01%. As we could be making some errors in our estimate of the mass change or the area, we double our estimate of the mass change and we halve the area of the drainage basin. These changes should increase the contributions from the glaciers. However, the change in our estimate of Z caused by adding these glacier signals to the SMB fields, remains at only 0.01%. We conclude that present day mass changes on these glaciers will not change our estimate of Z outside of the error bars already assigned.

Table 1 summarizes the values that we obtain for Z for the RACMO2 and altimetry cases discussed. The results indicate that Z determined from the weighted mean of the estimates from the RACMO2 SMB fields ($Z_{RACMO2} = -0.274$ including calculations with and without the elevation of the mass change) and $Z_{ALT} = -0.280$ are consistent to within the error bars. Considering the time period of our absolute gravity and GPS observations as well as the time period of the altimetry estimate for Z, we will form a weighted average of the last two values in Table 1 such that our best estimate for Z is $Z = -0.279 \pm 0.01$ μGal/mm. This value will be used in Section 5 to derive the GIA uplift rate at KULU. In Sections 3 and 4, we describe our uplift and gravity observations at KULU.

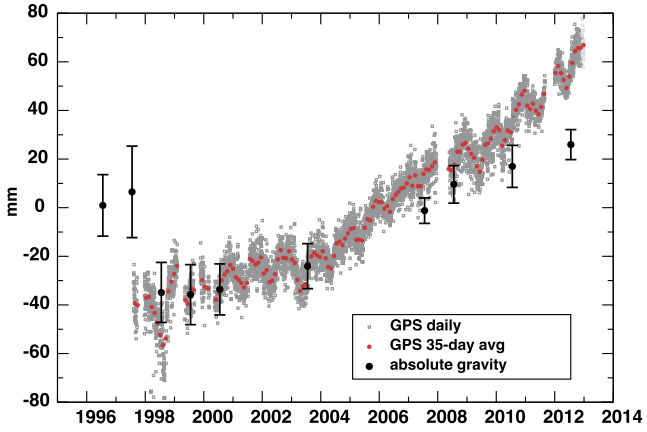

Fig. 3. Grey dots represent solution for the daily GPS up coordinate. The red dots are the 35-day averages of the GPS observations. Black circles with error bars represent the absolute gravity values converted to displacement using the free-air gravity gradient, −3.086 mm/μGal. The mean of the absolute gravity is deliberately adjusted so that the absolute gravity data between 1998 and 2000 fall on the GPS observations for that period.

3. GPS coordinate time series

In a joint effort, the National Oceanic and Atmospheric Administration, the University of Colorado, and the National Aeronautical and Space Administration's Program for Regional Climate Assessment (PARCA), installed a continuously operating GPS site at Kulusuk (KULU) in southeast Greenland, in 1996. We have processed the GPS data (see Bevis et al., 2012) to derive daily vertical positions of the KULU antenna.

The KULU daily height coordinate time series is shown in grey in Fig. 3. The GPS observations actually start in 1996, however we only use data between 1998.5 and 2012.5, i.e. only the GPS data that span the epochs of the absolute gravity observations. Changes in the up coordinate are related to seasonal and other short-period variations in environmental surface mass (atmospheric, oceanic, and continental water mass including snow and ice), long-period present-day ice-mass changes, and secular uplift/subsidence related to GIA.

The daily positions are not entirely random, however. They arise from a combination of measurement errors and mismodeled signal. The 1-sigma formal errors output by the GAMIT software do not include orbit errors, tropospheric modelling errors, or multipath errors. A more realistic error can be obtained using the method outlined in Wahr et al. (2001) and Khan et al. (2007).

To estimate more realistic errors on the GPS trends, we determine the decorrelation time of the data set, i.e. when the auto correlation drops to 0. As in Wahr et al. (2001) we determine that the decorrelation is between 30 and 50 days. We choose a decorrelation time of 35 days to construct multiday averaged. This averaging time represents a compromise between longer averaging times that would minimize the correlated errors and short averaging times to take advantage of the fact that much of the error in the daily observations is random. These 35-day averages are then used to construct the error estimates.

The velocities we determine from the GPS data depend on the errors we assign to each 35-day average. We assign the error using the scatter of the residuals about the mean of each of the 35-day averages. The errors on the 35-day averages range between 2.0 and 5.0 mm.

The GPS uplift rates are provided in the ITRF08 reference frame, that is equivalently a Center of Figure reference frame. The uncertainty in the scale rate for ITRF 2008 is 0.15 mm/yr (Z. Altamimi, 19-April, 2016, personal communication). We add this uncertainty in quadrature to each of the 35-day averages.

Table 2
Observed trends in absolute gravity and the GPS up coordinate; GIA determined from the observations. GPS trends represent the fits using the 35-day average trends.

Temporal range of fit	Absolute g (μGal/yr)	GPS up (mm/yr)	GIA up (mm/yr)	Elastic up (mm/yr)
1998.5–2003.5	-0.19 ± 0.29	3.37 ± 0.55	6.10 ± 2.78	-1.12 ± 1.54
2003.5–2012.5	-1.95 ± 0.16	8.71 ± 0.13	3.90 ± 1.68	4.22 ± 1.44
Weighted average			4.49 ± 1.44	

The rate of GPS uplift over the period investigated is somewhat variable (Fig. 3). The uplift from 1998 to 2003 is small and begins to increase in the summer of 2003. This increase is also observed in uplift time series from other long-term observing GPS sites in Greenland (Jiang et al., 2010), and in the GRACE gravity fields (Rignot et al., 2011) indicating that the mass loss over much of the GrIS began to accelerate in this time.

Our ability to separate the present day melting signal from the GIA signal according to the theory presented in Section 2, relies on our ability to extract precise velocities from the input data. Given the obvious change in the rate of uplift we will estimate the velocity for two different periods, and we will constrain our estimates of the uplift trends to the time periods of the absolute gravity data. The two periods that we use to determine the GIA signal are 1998.5–2003.5 and 2003.5–2012.5. (As our theory relies on precise estimates of the absolute gravity and GPS trends, if we fit a trend to the entire period, 1998.5–2012.5, the change in the uplift rate will introduce a large and unrealistic error to our estimates.) The rates of uplift for these two periods are given in Table 2 Column 3. (Even though we have GPS data going back to 1997 at KULU, we compute the trends using the data beginning in 1998.5 to coincide with the time periods of the gravity observations. See the following section.)

Any trend in surface mass loading not included in the present day changes in ice mass will contribute to the trend in the observed GPS uplift trends. Environmental surface loads include temporal and spatial redistribution of atmospheric, non-tidal ocean, and continental water mass. We predict the trends in atmospheric mass loading by determining the loading at KULU due to global surface pressure changes. To determine this trend, we use the 6-hourly data from the National Center for Environmental Prediction Reanalysis data set convolved with mass loading Green's functions to determine the surface displacement at KULU (van Dam and Wahr, 1987). For the two time periods, 1998.5–2003.5 and 2003.5–2012.5, we estimate that the atmosphere contributes a trend of .01 and .02 mm/yr respectively. These trends are assumed to be uncertainties in our GPS trend estimate and are added in quadrature to the errors on trends determined using the 35-day averages. The values reported in Table 2 Column 3 include these errors.

Estimating a temporal trend in non-tidal ocean loading using output from general ocean circulation models is difficult as these models use the Boussinesq approximation, i.e. oceanic volume and not mass is conserved in the model (Ponte et al., 2007). Thus, it would be difficult to distinguish a trend due to a true change in mass versus a change in trend due to conserving volume.

We compare our uplift rates (3.37 ± 0.55 and -8.71 ± 0.13 mm/year for the two time periods) to the rates predicted by the SMB. RACMO2 SMB predict that the Earth's surface at KULU should have uplifted at a rate of 0.88 ± 0.07 mm/yr for the period 1998.5 to 2003.5 and then at a higher rate of 1.72 ± 0.07 mm/yr for 2003.5 to 2012.5. The SMB rates are much slower than the observed rates of uplift for the same two periods. As the GIA uplift is constant for both periods, the increased rate of uplift near Kulusuk must be due to other process. Recall that RACMO2 only

calculates SMB, it does not account for the dynamic effects of glaciers, i.e. advance and retreat of the grounding line or increased discharge. The increased rate of after 2003 has been shown to be due to mass loss from the Helheim Glacier located ∼90 km to the northwest of the GPS station (Khan et al., 2007; Wahr et al., 2013) with some contributions coming from mass loss of the Midgaard and Kangerdlugssuaq glaciers (Wahr et al., 2013). Both Helheim and Kangerdlugssuaq experienced significant increases in velocity and thinning in 2003 and 2004 (Howat et al., 2011; Khan et al., 2014), the period when our GPS up coordinate changes velocity.

4. Absolute gravity time series

The absolute gravity data processing follows the protocol adopted during absolute gravimeters comparisons at the BIPM in Sèvres (Francis and van Dam, 2003). Geophysical corrections are applied to the raw gravity data: Earth and ocean tides, atmospheric pressure effect and the polar motion effect using pole positions from the International Earth Rotation Service. As there are no gravity tide observations are available in Kulusuk, the tidal prediction is based on an Earth tide model (Dehant et al., 1999) plus the computed ocean loading and attraction effects using the Schwiderski oceanic tides maps using the method outlined in Francis and Mazzega (1990). More recent oceanic tidal models were tested. The results were not improved as Kulusuk is only a few meters from the shoreline and the models tend to be reliable further away from the coast. To reduce the errors due to the tides, the gravity data are averaged over 24 hours. Atmospheric effects are modeled using a linear admittance factor of −3.0 μGal/hPa. The Polar motion effects are removed using the formulation of Wahr (1985) based on the International Earth Rotation Service daily estimates of the pole position (http://hpiers.obspm.fr). The *g-soft* version 9.0 software from *Microg-LaCoste Inc.* was used for the processing.

The uncertainties are the root square sum of the mean set standard deviation and are constant depending of the period of the measurements. An additional uncertainty of 2 μGals has been added to the measurements taken before 2001 to account for the fact that we used different gravimeters before 2001 and same instrument, FG5-216, afterward. The 2 μGals here corresponds to the accuracy specification of the manufacturer of the FG5 and has been confirmed during International Comparisons of Absolute Gravimeters (see for example, Francis et al., 2015). An offset was detected between 2002 and 2008 in the FG5-216 observations. Thus, the observations have been corrected for this offset.

Fig. 3 shows the absolute gravity data superimposed on the GPS up coordinate observations. The gravity observations have been multiplied by the free-air gravity gradient, −3.086 mm/μGal, to convert gravity to millimeters of uplift. (We apply the free-air gravity gradient only for a visual comparison of the two series in the figure and not for calculations presented in the text except where specified.)

With respect to the 1996 and 1997 gravity outliers, a hotel was constructed in 1997 less than 10 meters away and downhill from our absolute gravity point. The extra mass of the hotel causes the gravity after the construction to be higher than before. As it is not possible to precisely estimate the mass and the mass distribution of the Kulusuk Hotel, we ignore the gravity values taken before 1998.

Even after ignoring the anomalous gravity values collected in 1996 and 1997, the free-air corrected gravity observations exhibit different trends before and after 2003.5. However, the exact epoch of the change in trend is difficult to determine due to the lack of gravity observations at this time. We list the rates of change in gravity for the two time spans, in Table 2 Column 2.

In the next section, we use the estimates of uplift and gravity change rates to estimate the GIA signal at Kulusuk using the theory presented in Section 2.

5. Estimates of GIA and present day mass change

In this section, we estimate the GIA uplift rate, $\delta\dot{u}_{GIA}$, at KULU using the absolute gravity and GPS up trends provided in Table 2, and the value of $Z = -0.279 \pm 01$ estimated in Section 2 (a summary of all the Z calculations is provided in Table 1). We use these observations in Equation (6) to estimate the values of $\delta\dot{u}_{GIA}$ given in Table 2 Column 4. We derive the uncertainties for $\delta\dot{u}_{GIA}$ by propagating the uncertainties on the observed gravity and uplift trends and Z in Equation (6). Specifically, the variance on $\delta\dot{u}_{GIA}$ is determined using

$$\sigma^2_{\delta\dot{u}_{GIA}} \simeq \sigma^2_{\dot{u}}\left[\frac{\partial(\delta\dot{u}_{GIA})}{\partial(\delta\dot{u})}\right]^2 + \sigma^2_{\dot{g}}\left[\frac{\partial(\delta\dot{u}_{GIA})}{\partial(\delta\dot{g})}\right]^2 + \sigma^2_{z}\left[\frac{\partial(\delta\dot{u}_{GIA})}{\partial(\delta Z)}\right]^2.$$

The original uncertainties on the absolute gravity are observational uncertainties that are assigned by the absolute gravity data processing software. The errors on the 35-day GPS height coordinates are described in Section 3.

There are two things to note about our estimates for $\delta\dot{u}_{GIA}$ that are presented in Column 4 of Table 2. First, all estimates for $\delta\dot{u}_{GIA}$ are positive, i.e. they predict uplift. And second, our estimates of $\delta\dot{u}_{GIA}$ are much larger than their uncertainties.

The average GIA uplift rate at KULU, determined by calculating the weighted average of the values in Table 2 Column 4, is 4.49 ± 1.44 mm/yr. However, we would like to determine whether our infrequent and irregular gravity observations could bias our estimate of the secular trend in gravity, to the extent that it might have a significant effect on our estimate of $\delta\dot{u}_{GIA}$. In other words, we test if we would have obtained a different estimate of $\delta\dot{u}_{GIA}$ if we had truly continuous, daily gravity observations, instead of an incomplete set of quasi-yearly observations. To set up this test, we generate two new time series of synthetic gravity data. First, we generate a GIA-free uplift time series by removing a weighted mean of the values of $\delta\dot{u}_{GIA}$ in Table 2 from the 35-day uplift observations (this mean value is $\delta\dot{u}_{GIA} = 4.49 \pm 1.44$ mm/yr). We then multiply these 35-day uplift data by $Z = -0.279$ μGal/mm to generate a synthetic 35-day time series of gravity data. For the second data set, we extract gravity from our 35-day gravity time series but only at the epochs of our actual FG5 observations. We fit a line to both time series and compare the trends. Further, because of the acceleration in the uplift after 2003.5, we only use data after 2003.5 for this test. For the 35-day gravity values, we get a trend of −1.22 μGal/yr. For the time series where we epoch gravity observations, we get a value of −1.31 μGal/yr. The difference between these trends is about 0.11 μGal/yr, a difference that is smaller than the formal error on our weighted average for $\delta\dot{u}_{GIA}$.

We can now use our estimate of $\delta\dot{u}_{GIA}$ in Equation (1a) along with the GPS result for the total uplift rate to estimate the uplift rate due to present day mass changes. Estimates for $\delta\dot{u}_{ice}$ are given in the last column of Table 2 for the two time periods.

What about the uplift due to present day melting? Using the approach outlined in this paper, we predict that before 2000, the recent ice mass load was increasing, and KULU was subsiding. Subsidence at KULU for this period is also predicted using the RACMO2 SMB model (not shown). Box et al. (2004), Box (2006) use high-resolution climate models to demonstrate that for the period 1980–2000 the SMB anomaly in the region of KULU was positive.

After the summer of 2003, our calculations indicate that the surface load was decreasing and the site uplifted. This modeled

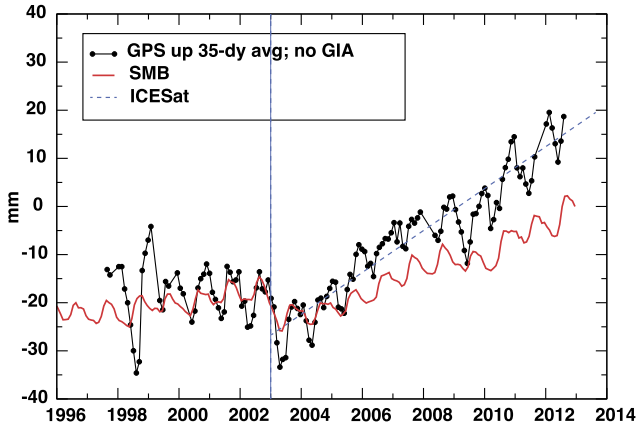

Fig. 4. A comparison of our GPS time series with GIA removed (black) and vertical surface displacement predicted using RACMO2 (red) at KULU. The dashed blue line represents the surface displacement predicted by the ice volume change derived primarily from ICESat that is valid from 2003 (vertical dashed line) extended in time for visual comparison only.

elastic uplift for this later period is also consistent with models and other observations that indicate that mass loss accelerated sometime in the summer of 2003 (Zwally et al., 2011; Murray et al., 2010; Bevan et al., 2012). Further, Howat et al. (2007, 2008) show that the Helheim glacier began to accelerate and thin in 2003. The rapid discharge of Helheim would also cause an uplift at KULU (Khan et al., 2007).

6. Comparison with models

We can use our improved estimate of $\delta\dot{u}_{ice}$, the elastic uplift at KULU, to assess models of the present day ice mass change. In Fig. 4, we compare our observed uplift at KULU (black dots), after removing a 4.49 ± 01.44 mm/yr GIA trend (GIA was computed by averaging the two values in Table 2 Column 4 and including the GIA error resulting from using quasi-annual versus daily gravity observations. See Section 5). Also shown in Fig. 4 is the predicted elastic uplift using the RACMO SMB output (red line). For the discussion in this section, we will only comment on the data after 2003.5 as these data have the lowest observational errors on the uplift.

The slope of the GIA-free uplift observations for the period 2003.5–2012.5 is 4.22 ± 1.44 mm/yr (Table 2 Column 5). The estimate of the uplift from the SMB model for the same period is 1.72 ± 0.07 mm/yr. There is a larger trend in the GPS up observations than in the SMB model, and this perhaps indicates that mass loss at KULU at that time was affected by mass loss on the nearby glaciers. If we assume that the difference in slope between the SMB and GIA-free observations is due to glacier dynamics, and we assume all the uplift is from mass loss on the Helheim Glacier, then from 1997 to 2003 we estimate that Helheim is losing ice-mass at a rate of about 10 km^3/yr. To determine this rate of mass loss, we put a disk load with a radius of the Helheim glacier basin at the location of the glacier. Then we use mass loading Green's functions to determine that the mass loss must be the order of 10 km^3/yr. This estimate, quantitatively, compares well with the 14–16 km^3/yr estimated by Howat et al. (2008) and others. However, our mass loss estimate should be interpreted carefully. Our estimate of mass loss on Helheim is based on a single data point and a number of assumptions that include constraining all the mass loss to the Helheim drainage basin when in fact some of the mass loss may be coming from Kangerdlugssuaq or other nearby glaciers.

How does our estimate of GIA compare with previously published estimates of GIA from the Kulusuk region? Predictions of $\delta\dot{u}_{GIA}$ computed using the global ICE-5G deglaciation model and VM2 viscosity profile (lithospheric thickness = 90 km; upper mantle viscosity = 0.5×10^{21} Pa s; lower mantle viscosity = 2.7×10^{21} Pa s), one of a number of radially symmetric depth dependent mantle viscosity models (Peltier, 2004), suggest that the GIA uplift rate at KULU is −0.12 mm/yr. Using the ANU05 (lower) ice history model and a slightly different viscosity model that, the predicted uplift rate due to GIA is −1.16 mm/yr (Spada et al., 2012). (Other estimates of GIA at Kulusuk for different Earth models calculated by Spada et al. (2012) are provided in Table 3.) A et al. (2013) modeled the global GIA signal using the ICE-5G deglaciation model and the VM2 viscosity profile, but correcting an error in the way Peltier included the effects of GIA-induced polar wander. A et al. obtained a GIA uplift rate at KULU of −0.7 mm/yr. The models and rates described above are summarized in Table 3.

Recall that our estimates of GIA from both time periods are positive and that they almost agree with one another to within the error bars. The disagreement between our GIA estimates and the GIA from the models indicates that there may still be errors in the ice model or the viscosity profile. More importantly these model predictions differ from our estimates of $\delta\dot{u}_{GIA}$ by more than the error on our estimates.

7. Discussion

By combining infrequent absolute gravity and 35-day averaged uplift from daily observations at Kulusuk, Greenland, we estimate the GIA uplift trend for that location. Our observations indicate that the Earth's surface is rebounding upwards in the vicinity of KULU, a result that disagrees with most models of GIA for the region that predict that the lithosphere at KULU should be subsiding (see Table 3). GIA models are comprised of a sea-level model, a model of ice sheet mass change through time, and a model of Earth rheology. The disagreement of our observations with most existing model predictions is most likely due to insufficient knowledge of the ice extent at the LGM and the deglaciation history of the ice in southeast Greenland. However, our GIA uplift rate at KULU, 4.49 ± 1.44 mm/yr is consistent with recent GIA uplift rate of 4.4 ± 0.1 mm/yr by Khan et al. (2016). While we use GPS and gravity measurements to separate GIA from elastic uplift, Khan et

Table 3
Summary of the Earth and Ice models used to determine GIA. LT = Lithospheric thickness; UM v = Upper mantle viscosity; LM v = Lower mantle viscosity.

	LT (km)	UM v ($\times 10^{21}$ Pa s)	LM v ($\times 10^{21}$ Pa s)	Ice model	Uplift (mm/yr)
Peltier (2004)	90	0.5	2.7	ICE-5G	−0.12
From Table 2-3 Spada et al. (2012)	50	0.2	5.0	ANU05	−1.16
From Table 2-3 Spada et al. (2012)	80	0.4	10	ANU05	−2.02
From Table 2-3 Spada et al. (2012)	100	0.5	20	ANU05	−1.74
From Table 1 Simpson et al. (2011)	120	5	10	HUY2	0.41
From Table 1 Simpson et al. (2011)	120	3.0	50	HUY2 East	−1.23
From Table 1 and S1 Khan et al. (2016)	40–60	0.5	20	Modified ANU05	4.4 ± 0.1
This paper					4.49 ± 1.44

al. use a different approach. They estimate the elastic uplift using satellite altimetry data.

The deglaciation history of southeast Greenland is difficult to quantify because relative sea level observations (RSL) from large sections of the GrIS margin do not exist (Roberts et al., 2008). RSL observations in southeast Greenland are particularly sparse (Fleming and Lambeck, 2004; Tarasov and Peltier, 2002; Long et al., 2008; Roberts et al., 2008). In fact, Fleming and Lambeck (2004) do not use any relative sea level histories from this region to develop their LGM deglaciation history (ANU05). Their ice-extent model for this region extends only moderately onto the continental shelf and indicates an ice thickness change of 500–1000 m along the present day south eastern Greenland coast.

Tarasov and Peltier (2002) developed another relative sea level inversion for the Greenland deglaciation history. Their LGM model is thicker than that of the Fleming and Lambeck (2004) model with maximum thicknesses in southeast Greenland of 800–1200 m. However, the authors indicate that due to the lack of relative sea level histories from this region, their results here are not well constrained.

Huybrechts (2002) developed another model (independent of sea level histories) suggesting that the thickness during the LGM was up to 1500 m in southeast and that the ice extended 200 km further (from the present day coastline) onto the continental shelf than predicted by Tarasov and Peltier (2002).

Isolation basin derived reconstructions of RSL by Long et al. (2008) support the idea of an even thicker ice model with an even greater extension of the ice sheet onto the continental shelf during the LGM than the models by Huybrechts (2002), Tarasov and Peltier (2002), and Fleming and Lambeck (2004). This result is supported by Roberts et al. (2008) who use trim line mapping to conclude that the ice was at least 740 m thick over the current coastline and that deglaciation in the region near Kulusuk was very rapid and started relatively late, 11–9.5 ky BP.

A newer ice history reconstruction by Simpson et al. (2009), Huy2, tuned to fit the RSL data extends the LGM ice further onto the continental shelf than the model presented in Huybrechts (2002). Simpson et al. (2011) use Huy2 to predict the present day viscoelastic vertical crustal velocities around Greenland for two Earth models: a best fit Earth model (lithospheric thickness = 120 km; upper mantle viscosity = 5×10^{20} Pa s; lower mantle viscosity = 1.0×10^{21} Pa s) and a best fit Earth model for eastern Greenland (lithospheric thickness = 120 km; upper mantle viscosity = 3×10^{20} Pa s; lower mantle viscosity = 50×10^{21} Pa s). In the region of Kulusuk, Simpson et al. (2011) predict viscoelastic uplift rates of 0.41 and −1.23 mm/yr for the two Earth models (Table 3). The viscoelastic uplift predicted by these authors is primarily sensitive to upper mantle viscosity. S-wave velocities are slower than average at depths down to 630 km (Steigenberger et al., 2015) indicating that the upper mantle is hotter than average under southeast Greenland. A warmer upper mantle would reduce the viscosity and might even produce a greater viscoelastic uplift in south-east Greenland than predicted in Simpson et al. (2011).

Our observation of GIA uplift at Kulusuk is still greater than the only positive estimate of GIA from the region. Therefore, our estimate of GIA supports the idea of a thicker ice sheet that extended onto the shelf (Simpson et al., 2009) and/or a less viscous upper mantle.

Our single GIA trend at Kulusuk does not allow us to estimate the present day rate of mass loss over the entire Greenland ice sheet. For that, we would need long time series of absolute gravity observations co-located with GPS at many sites. However, our GIA trend does provide a new data point for testing future models of GIA (ice history + Earth model). If our ice model is perfect, then we can use out observed GIA to improve the Earth model. Similarly, if the Earth model were perfect, our observation would help constrain the ice history. Furthermore, our estimate of the elastic surface displacement KULU is an improvement over previous estimates, because we can now remove a more reliable GIA signal. This improved estimate of the elastic uplift can be used to test new linear ice mass change models.

References

A, G., Wahr, J., Zhong, S., 2013. Computations of the viscoelastic response of a 3-D compressible Earth to surface loading: an application to Glacial Isostatic Adjustment in Antarctica and Canada. Geophys. J. Int. 192 (2), 557–572. http://dx.doi.org/10.1093/gji/ggs030.

Argus, D., Peltier, W.R., Drummond, R., Moore, A.W., 2014. The Antarctica component of postglacial rebound model ICE-6G_C (VM5a) based on GPS positioning, exposure age dating of ice thicknesses, and relative sea level histories. Geophys. J. Int. 198 (1), 537–563. http://dx.doi.org/10.1093/gji/ggu140.

Bevan, S.L., Luckman, A.J., Murray, T., 2012. Glacier dynamics over the last quarter of a century at Helheim, Kangerdlugssuaq and 14 other major Greenland outlet glaciers. Cryosphere 6, 1637–1672. http://dx.doi.org/10.5194/tcd-6-1637-2012. www.the-cryosphere-discuss.net/6/1637/2012/.

Bevis, M., Wahr, J., Khan, S.A., Madsen, F.B., Brown, A., Willis, M., Kendrick, E., Knudsen, P., Box, J.E., van Dam, T., Caccamise II, D.J., Johns, B., Nylen, T., Abbot, R., White, S., Miner, J., Forsberg, R., Zhou, H., Wang, J., Wilson, T., Bromwich, D., Francis, O., 2012. Bedrock displacements in Greenland manifest ice mass variations, climate cycles and climate change. Proc. Natl. Acad. Sci. USA 109, 11944–11948. http://dx.doi.org/10.1073/pnas.1204664109.

Box, J.E., 2006. Greenland ice sheet surface mass balance variability: 1991–2003. Ann. Glaciol. 42, 42A142.

Box, J.E., Bromwich, D.H., Bai, L.-S., 2004. Greenland ice sheet surface mass balance 1991–2000: application of Polar MM5 mesoscale model and in situ data. J. Geophys. Res. 109, D16105. http://dx.doi.org/10.1029/2003JD004451.

Csatho, B., Schenka, M.A.F., van der Veen, C.J., Babonis, G., Duncan, K., Rezvanbehbahani, S., van den Broeke, M.R., Simonsen, S.B., Nagarajan, S., van Angelen, J.H., 2014. Laser altimetry reveals complex pattern of Greenland Ice sheet dynamics. Proc. Natl. Acad. Sci. 111, 18478–18483. http://dx.doi.org/10.1073/pnas.1411680112.

Dehant, V., Defraigne, P., Wahr, J.M., 1999. Tides for a convective Earth. J. Geophys. Res. 104 (B1), 1035–1058.

Dziewonski, A., Anderson, D.L., 1981. Preliminary reference Earth model. Phys. Earth Planet. Inter. 25, 297–356.

Ettema, J., van den Broeke, M.R., van Meijgaard, E., van de Berg, W.J., Bamber, J.L., Box, J.E., Bales, R.C., 2009. Higher surface mass balance of the Greenland ice sheet revealed by high resolution climate modeling. Geophys. Res. Lett. 36, L12501. http://dx.doi.org/10.1029/2009GL038110.

Ewert, H., Groh, A., Dietrich, R., 2012. Volume and mass changes for the Greenland ice sheet inferred from ICESat and GRACE. J. Geodyn. 59–60, 111–123. http://dx.doi.org/10.1016/j.jog.2011.06.003.

Farrell, W., 1972. Deformation of the Earth by surface loads. Rev. Geophys. Space Phys. 10, 761–797.

Fleming, K., Lambeck, K., 2004. Constraints on the Greenland ice sheet since the Last Glacial Maximum from sea-level observations and glacial-rebound models. Quat. Sci. Rev. 23, 1053–1077. http://dx.doi.org/10.1016/j.quascirev.2003.11.001.

Francis, O., van Dam, T.M., 2003. Processing of the absolute data of the ICAG01. Cah. Cent. Eur. Géodyn. Séismol. 22, 45–48.

Francis, O., Mazzega, 1990. Global charts of ocean tide loading effects. J. Geophys. Res. 95 (C7), 11411–11424.

Francis, O., Baumann, H., Ullrich, C., Castelein, S., Van Camp, M., Sousa, M.A., Melhorato, R.L., Li, C., Xu, J., Su, D., Wu, S., Hu, H., Wu, K., Li, G., Li, Z., Hsieh, W.-C., Pálinkás, P.V., Kostelecký, J., Mäkinen, J., Näränen, J., Merlet, S., Santos, F.P.D., Gillot, P., Hinderer, J., Bernard, J.-D., Moigne, N.L., Fores, B., Gitlein, O., Schilling, M., Falk, R., Wilmes, H., Germak, A., Biolcati, E., Origlia, C., Iacovone, D., Baccaro, F., Mizushima, S., De Plaen, R., Klein, G., Seil, M., Radinovic, R., Sekowski, M., Dykowski, P., Choi, I.-M., Kim, M.-S., Borreguero, A., Sainz-Maza, S., Calvo, M., Engfeldt, A., Agren, J., Reudink, R., Eckl, M., Westrum, D.V., Billson, R., Ellis, B., 2015. CCM.G-K2 key comparison. Metrologia 52 (1A).

Howat, I.M., Joughin, I.R., Scambos, T.A., 2007. Rapid changes in ice discharge from Greenland outlet glaciers. Science 315, 1559–1561.

Howat, I.M., Smith, B.E., Joughin, I., Scambos, T.A., 2008. Rates of southeast Greenland ice volume loss from combined ICESat and ASTER observations. Geophys. Res. Lett. 35, L17505. http://dx.doi.org/10.1029/2008GL034496.

Howat, I.M., Ahn, Y., Joughin, I., van den Broeke, M.R., Lenaerts, J.T.M., Smith, B., 2011. Mass balance of Greenland's three largest outlet glaciers, 2000–2010. Geophys. Res. Lett. 38, L12501. http://dx.doi.org/10.1029/2011GL047565.

Huybrechts, P., 2002. Sea-level changes at the LGM from ice-dynamic reconstructions of the Greenland and Antarctic ice sheets during the glacial cycles. Quat. Sci. Rev. 21, 203–231. http://dx.doi.org/10.1016/S0277-3791(01)00082-8.

Jiang, Y., Dixon, T., Wdowinski, S., 2010. Accelerating uplift in the North Atlantic region as an indicator of ice loss. Nat. Geosci. 3, 404–407. http://dx.doi.org/10.1038/ngeo845.

Khan, S.A., Wahr, J., Stearns, L.A., Hamilton, G.S., van Dam, T., Larson, K.M., Francis, O., 2007. Elastic uplift in southeast Greenland due to rapid ice mass loss. Geophys. Res. Lett. 34, L21701. http://dx.doi.org/10.1029/2007GL031468.

Khan, S.A., Wahr, J., Bevis, M., Velicogna, I., Kendrick, E., 2010. Spread of ice mass loss into northwest Greenland observed by GRACE and GPS. Geophys. Res. Lett. 37, L06501. http://dx.doi.org/10.1029/2010GL042460.

Khan, S.A., et al., 2013. Recurring dynamically induced thinning during 1985 to 2010 on Upernavik Isstrøm, West Greenland. J. Geophys. Res., Earth Surf. 118, 111–121. http://dx.doi.org/10.1029/2012JF002481.

Khan, S.A., Kjeldsen, K.K., Kjær, K.H., Bevan, S., Luckman, A., Aschwanden, A., Bjørk, A.A., Korsgaard, N.J., Box, J.E., van den Broeke, M., van Dam, T.M., Fitzner, A., 2014. Glacier dynamics at Helheim and Kangerdlugssuaq glaciers, southeast Greenland, since the Little Ice Age. Cryosphere 8, 1497–1507. http://dx.doi.org/10.5194/tc-8-1497-2014.

Khan, S.A., Sasgen, I., Bevis, M., van Dam, T., Bamber, J.L., Wahr, J., Willis, M., Kjær, K.H., Wouters, B., Helm, V., Csatho, B., Fleming, K., Bjørk, A.A., Aschwanden, A., Knudsen, P., Munneke, P.K., 2016. Geodetic measurements reveal similarities between Last Glacial Maximum and present-day mass loss from the Greenland ice sheet. Sci. Adv. 2, e1600931.

Kjeldsen, K.K., Khan, S.A., Wahr, J., Korsgaard, N.J., Kjær, K.H., Bjørk, A.A., Hurkmans, R., van den Broeke, M.R., Bamber, J.L., van Angelen, J.H., 2013. Improved ice loss estimate of the northwestern Greenland ice sheet. J. Geophys. Res. 118. http://dx.doi.org/10.1029/2012JB009684.

Krabill, W.B., 2011. IceBridge ATM L2 Icessn Elevation, Slope, and Roughness, [1994–2010]. National Snow and Ice Data Center, Boulder, Colo.

Long, A.J., Woodroffe, S.A., Dawson, S., Roberts, D.H., Bryant, C.L., 2008. Late Holocene relative sea level rise and the Neoglacial history of the Greenland ice sheet. J. Quat. Sci. 24, 345–359. http://dx.doi.org/10.1002/jqs.1235.

Mémin, A., Hinderer, J., Rogister, Y.Y., 2012. Separation of the geodetic consequences of past and present ice-mass change: influence of topography with application to Svalbard (Norway). Pure Appl. Geophys. 169 (8), 1357–1372.

Murray, T., et al., 2010. Ocean regulation hypothesis for glacier dynamics in Southeast Greenland and implications for ice sheet mass changes. J. Geophys. Res. 115, F03026. http://dx.doi.org/10.1029/2009JF001522.

Nielsen, K., Khan, S.A., Korsgaard, N.J., Kjær, K.H., Wahr, J., Bevis, M., Stearns, L.A., Timm, L.H., 2012. Crustal uplift due to ice mass variability on Upernavik Isstrøm, west Greenland. Earth Planet. Sci. Lett. 353–354, 182–189. http://dx.doi.org/10.1016/j.epsl.2012.08.024.

Noël, B., van de Berg, W.J., van Meijgaard, E., Kuipers Munneke, P., van de Wal, R.S.W., van den Broeke, M.R., 2015. Evaluation of the updated regional climate model RACMO2.3: summer snowfall impact on the Greenland Ice Sheet. Cryosphere 9 (5), 1831–1844. http://dx.doi.org/10.5194/tc-9-1831-2015.

Peltier, W.R., 2002. On eustatic sea level history, Last Glacial Maximum to Holocene. Quat. Sci. Rev. 21, 377–396. http://dx.doi.org/10.1016/S0277-3791(01)00084-1.

Peltier, W.R., 2004. Global glacial isostasy and the surface of the ice-age Earth: the Ice-5g (VM2) Model and GRACE. Annu. Rev. Earth Planet. Sci. 32, 111–149. http://dx.doi.org/10.1146/annurev.earth.32.082503.144359.

Ponte, R., Quinn, K., Wunsch, C., Heimbach, P., 2007. A comparison of model and GRACE estimates of the large-scale seasonal cycle in ocean bottom pressure. Geophys. Res. Lett. 34. http://dx.doi.org/10.1029/2007GL029599.

Rignot, E., Kanagaratnam, P., 2006. Changes in the velocity structure of the Greenland Ice Sheet. Science 311, 986–990. http://dx.doi.org/10.1126/science.1121381.

Rignot, E., Velicogna, I., van den Broeke, M.R., Monaghan, A., Lenaerts, J., 2011. Acceleration of the contribution of the Greenland and Antarctic ice sheets to sea level rise. Geophys. Res. Lett. 38, L05503. http://dx.doi.org/10.1029/2011GL046583.

Roberts, D.H., Long, A.H., Schnabel, C., Freeman, S., Simpson, M.J.R., 2008. The deglacial history of southeast sector of the Greenland Ice Sheet during the Last Glacial Maximum. Quat. Sci. Rev. 27, 1505–1516. http://dx.doi.org/10.1016/j.quascirev.2008.04.008.

Siegfried, M.R., Hawley, R.L., Burkhart, J.F., 2011. High-resolution ground-based GPS measurements show intercampaign bias in ICESat elevation data near Summit, Greenland. IEEE Trans. Geosci. Remote Sens. 49, 3393–3400. http://dx.doi.org/10.1109/tgrs.2011.2127483.

Simpson, M.J.R., Milne, G.A., Huybrechts, P., Long, A.J., 2009. Calibrating a glaciological model of the Greenland ice sheet from the Last Glacial Maximum to present-day using field observations of relative sea level and ice extent. Quat. Sci. Rev. 28, 1631–1657. http://dx.doi.org/10.1016/j.quascirev.2009.03.004.

Simpson, M.J.R., Wake, L., Milne, G.A., Huybrechts, P., 2011. The influence of decadal- to millennial-scale ice mass changes on present-day vertical land motion in Greenland: implications for the interpretation of GPS observations. J. Geophys. Res. 116, B02406. http://dx.doi.org/10.1029/2010JB007776.

Smith, B.E., Fricker, H.A., Joughin, I.R., Tulaczyk, S., 2009. An inventory of active subglacial lakes in Antarctica detected by ICESat (2003–2008). J. Glaciol. 55, L21S09. http://dx.doi.org/10.3189/002214309789470879.

Spada, G., Ruggieri, G., Sørensen, L.S., Nielsen, K., Melini, D., Colleoni, F., 2012. Greenland uplift and regional sea level changes from ICESat observations and GIA modelling. Geophys. J. Int. 189. http://dx.doi.org/10.1111/j.1365-246X.2012.05443.x.

Steigenberger, B., Spakman, W., Japsen, P., Torsvik, T.H., 2015. The key role of global solid-Earth processes in preconditioning Greenland's glaciation since the Pliocene. Terra Nova 27. http://dx.doi.org/10.1111/ter.12133.

Tarasov, L., Peltier, W.R., 2002. Greenland glacial history and local geodynamic consequences. Geophys. J. Int. 150, 198–229.

van Dam, T.M., Wahr, J., 1987. Displacements of the Earth's surface due to atmospheric loading: effects on gravity and baseline measurements. J. Geophys. Res. 92, 1281–1286.

van den Broeke, M., et al., 2009. Partitioning recent Greenland mass loss. Science 326, 984–986. http://dx.doi.org/10.1126/science.1178176.

van Meijgaard, E., van Ulft, L.H., van de Berg, W.J., Bosveld, F.C., van den Hurk, B.J.J.M., Lenderink, G., Siebesma, A.P., 2008. The KNMI regional atmospheric climate model RACMO version 2.1. Technical report 302. Royal Netherlands Meteorological Institute (KNMI). 43 pp.

Wahr, John M., 1985. Deformation induced by polar motion. J. Geophys. Res., Solid Earth 90 (B11), 2156–2202. http://dx.doi.org/10.1029/JB090iB11p09363.

Wahr, J.M., van Dam, T., Larson, K., Francis, O., 2001. Geodetic Measurements in Greenland and their implications. J. Geophys. Res. 106, 16567–16581.

Wahr, J., Khan, S.A., van Dam, T., Liu, L., van Angelen, J.H., van den Broeke, M.R., Meertens, C.M., 2013. The use of GPS horizontals for loading studies, with applications to northern California and southeast Greenland. J. Geophys. Res., Solid Earth 118. http://dx.doi.org/10.1002/jgrb.50104.

Wahr, J., DaZhong, H., Trupin, A., 1995. Predictions of vertical uplift caused by changing polar ice volumes on a viscoelastic Earth. Geophys. Res. Lett. 22, 977–980.

Zwally, H.J., Brenner, A.C., Beckley, M., Cornejo, H.G., Dimarzio, J., Giovinetto, M.B., Neumann, T.A., Robbins, J., Saba, J.L., Donghui, Y., Wang, W., 2011. Greenland ice sheet mass balance: distribution of increased mass loss with climate warming; 2003–07 versus 1992–2002. J. Glaciol. 57 (201), 88–102.